Analysis of composite walls with and without openings

Autor(en): **Levy, Moshe / Spira, Ephraim**

Objekttyp: **Article**

Zeitschrift: **IABSE publications = Mémoires AIPC = IVBH Abhandlungen**

Band (Jahr): **33 (1973)**

PDF erstellt am: **27.05.2024**

Persistenter Link: https://doi.org/10.5169/seals-25623

Analysis of Composite Walls With and Without Openings

Analyse de parois en construction composite avec et sans ouvertures

Analyse von Verbundwänden mit und ohne Öffnungen

MOSHE LEVY
Lecturer in Civil Engineering, D.Sc., Research Fellow, Structural Dept. Building Research Station, Technion – Israel Institute of Technology

EPHRAIM SPIRA
Professor, Fac. of Civil Engineering Technion – Israel Institute of Technology

Introduction

Since some 20 years much research work has been devoted to the analysis of masonry walls with stiffening elements, which commonly occur in construction as load-bearing walls or shear walls.

A group of researchers chose an essentially experimental approach to investigate some specific aspects of the problem: the infilled frame [14]; the grade beam underneath the load-bearing wall [15]; the influence of openings, differential support settlements in continuous walls on heavy soils [1, 12].

Various analytical studies (occasionally in conjunction with experiments) based on the Finite-Elements-method appeared in the last decade [2, 7].

In spite of the obvious advantages of the Finite-Element method, a number of researchers preferred the analysis based on the Airy-stress function, which is particularly suitable for homogeneous walls without openings with given edge loadings. But in the authors' opinion their formulation of the compatibility conditions along the contact faces between plate and stiffening elements and of those required for walls with openings was not adequate. Therefore, the numerical solutions were obtained at the expense of tedious calculation of a basic system with too many degrees of freedom [4, 10, 15] or of neglecting the flexural rigidity of the stiffening elements [11].

The authors believe that their research study reported in [13] consolidated the elastic analysis of the composite wall. The main points of the proposed analysis as well as some conclusions resulting from particular cases solved numerically are given in the following.

Outline of the Analysis

The problem is essentially a boundary value problem in plane-stress elasticity and it is treated on the assumption that the masonry is isotropic and that the stiffeners obey the elementary beam theory; both are assumed to be linearly elastic, and considering its small effect, Poisson's ratio is neglected – $\nu = 0$ (in [9] orthotropy parameters for concrete hollow block masonry were experimentally investigated and were found to justify the above assumptions). For further simplification, the flexural rigidity of intermediate stiffeners is neglected (owing to the absence of external loading perpendicular to their axes) while that of the edge elements is allowed for in full.

The basic differential equation of the isotropic plate (with constant volume forces) is:

$$\frac{\partial^4 \Phi}{\partial x^4} + 2\frac{\partial^4 \Phi}{\partial x^2 \partial y^2} + \frac{\partial^4 \Phi}{\partial y^4} = 0, \tag{1}$$

the plate stresses being:

$$\sigma_y = \frac{\partial^2 \Phi}{\partial x^2}, \qquad \sigma_x = \frac{\partial^2 \Phi}{\partial y^2}, \qquad \tau = -\frac{\partial^2 \Phi}{\partial x \partial y}. \tag{2}$$

In Fig. 1 a plate edge of arbitrary shape and a stiffening element along part of it are shown. The external and the contact forces acting on the stiffener are also indicated. For an initial section (x_i, y_i) the values of the stress function Φ_i and of its derivatives $\left(\frac{\partial \Phi}{\partial x}\right)_i$, $\left(\frac{\partial \Phi}{\partial y}\right)_i$ are known.

At a location (s) on the unstiffened edge they are obtained from the known edge forces as follows:

$$\frac{\partial \Phi}{\partial y} = \frac{1}{t}\int_{s_i}^{s} X\,ds + \left(\frac{\partial \Phi}{\partial y}\right)_i, \qquad \frac{\partial \Phi}{\partial x} = -\frac{1}{t}\int_{s_i}^{s} Y\,ds + \left(\frac{\partial \Phi}{\partial x}\right)_i, \tag{3}$$

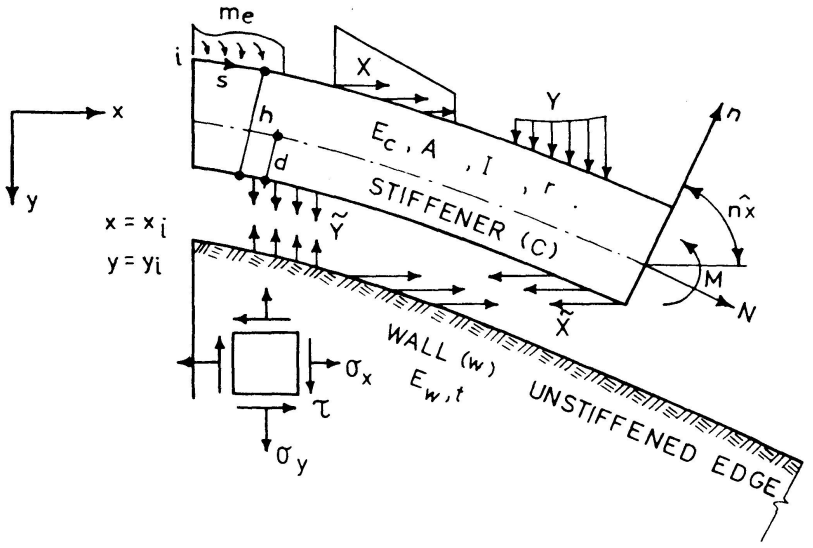

Fig. 1. Edge element and adjoining wall.

$$\Phi = \frac{1}{t}\int_{s_i}^{s}[X(y_s - y_i) + Y(x_i - x_s) + m_e]\,ds + \left(\frac{\partial \Phi}{\partial y}\right)_i y_s + \left(\frac{\partial \Phi}{\partial x}\right)_i x_s. \tag{3}$$

At the stiffened edges compatibility conditions expressing the equality of deformation of plate and stiffening element in both the tangential and perpendicular directions are set up. At a location(s) the inner forces of the stiffener due to external load and contact forces are found to be [13]:

$$N = N_e - t\frac{\partial \Phi}{\partial n}, \qquad M = M_e - t\left(d\frac{\partial \Phi}{\partial n} + \Phi\right). \tag{4}$$

N_e and M_e can readily be determined from the external loading, the stress function and its derivatives at an initial section ($s = s_i$), (which usually can be set equal to zero), and the edge geometry. They can be expressed as follows:

$$\begin{aligned} N_e &= \frac{dy}{dn}\left[t\left(\frac{\partial \Phi}{\partial y}\right)_i + \int_{s_i}^{s} X\,ds\right] + \frac{dx}{dn}\left[t\left(\frac{\partial \Phi}{\partial x}\right)_i - \int_{s_i}^{s} Y\,ds\right], \\ M_e &= t\left[\left(d\frac{dy}{dn} + y_s - y_i\right)\left(\frac{\partial \Phi}{\partial y}\right)_i + \left(d\frac{dx}{dn} + x_s - x_i\right)\left(\frac{\partial \Phi}{\partial x}\right)_i + \Phi_i\right] \\ &\quad + \int_{s_i}^{s}[X(y_s - y) + Y(x - x_s) + m_e]\,ds. \end{aligned} \tag{5}$$

The tangential compatibility condition is $u_c = u_w$ or

$$\frac{\partial u_c}{\partial s} = \frac{\partial u_w}{\partial s}, \quad \text{with } \nu_c = \nu_w = 0 \text{ leads to}$$

$$\frac{\sigma_c}{E_c} = \frac{\sigma_w}{E_w}, \quad \text{with } \sigma_c = \frac{M\,d}{I} + \frac{N}{A} \text{ and considering (4),}$$

we obtain

$$\Phi + d\left(1 + \frac{r^2}{d^2}\right)\frac{\partial \Phi}{\partial n} + \frac{E_c I}{E_w t\,d}\frac{\partial^2 \Phi}{\partial n^2} = \frac{1}{t}\left(M_e + N_e\frac{r^2}{d}\right). \tag{6}$$

The perpendicular compatibility conditions is $v_c = v_w$ or $\frac{\partial^2 v_c}{\partial s^2} = \frac{\partial^2 v_w}{\partial s^2}$; this can be expressed [13] as follows:

$$\Phi + d\frac{\partial \Phi}{\partial n} - \frac{E_c I}{E_w t}\left(\frac{\partial^3 \Phi}{\partial n^3} + 2\frac{\partial^3 \Phi}{\partial n\,\partial s^2}\right) = \frac{M_e}{t}. \tag{7}$$

As for internal stiffener (Fig. 2) the axial force is defined by:

$$N = N_e - t\left[\left(\frac{\partial \Phi}{\partial n}\right)_r + \left(\frac{\partial \Phi}{\partial n}\right)_l\right]. \tag{8}$$

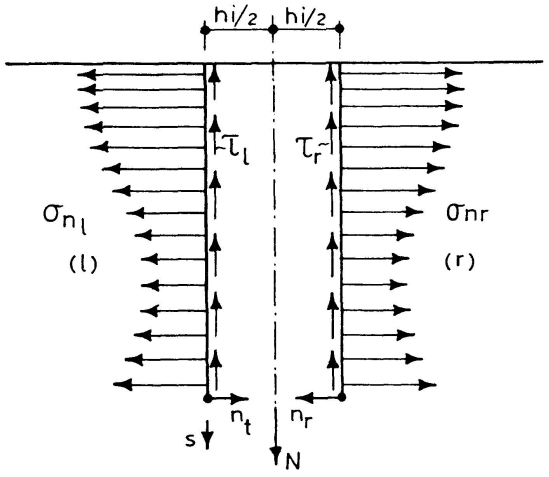

Fig. 2. Intermediate stiffener and adjoining wall.

The tangential compatibility conditions for either side of the stiffener are:

$$\left(\frac{\partial \Phi}{\partial n}\right)_l + \left(\frac{\partial \Phi}{\partial n}\right)_r + \frac{E_c A}{E_w t}\left(\frac{\partial^2 \Phi}{\partial n^2}\right)_r = \frac{N_e}{t},$$
$$\left(\frac{\partial \Phi}{\partial n}\right)_l + \left(\frac{\partial \Phi}{\partial n}\right)_r + \frac{E_c A}{E_w t}\left(\frac{\partial^2 \Phi}{\partial n^2}\right)_l = \frac{N_e}{t}. \tag{9}$$

As the flexural rigidity is neglected, the bending moment vanishes, i.e.:

$$M = t\left[-\left(\frac{h_i}{2}\frac{\partial \Phi}{\partial n} + \Phi\right)_r + \left(\frac{h_i}{2}\frac{\partial \Phi}{\partial n} + \Phi\right)_l\right] = 0,$$

or with $h_i \approx 0$

$$\Phi_l = \Phi_r. \tag{10}$$

Eq. (10) implies that normal stresses at both sides of air internal stiffener are equal.

The perpendicular compatibility condition at the internal stiffener – $(v_w)_1 = (v_w)_r$ yield, analogously to (7)

$$\left(\frac{\partial^3 \Phi}{\partial n^3} + 2\frac{\partial^3 \Phi}{\partial n\, \partial s^2}\right)_l = -\left(\frac{\partial^3 \Phi}{\partial n^3} + 2\frac{\partial^3 \Phi}{\partial n\, \partial s^2}\right)_r. \tag{11}$$

Statically Indeterminate Composite Walls

As the proposed method belongs to the category of the Flexibility Methods of the Theory of Structures, statical indeterminacy has to be dealt with in certain cases. In this paper such cases as walls continuous over more than two supports or infilled frames shall not be discussed in detail. Detailed treatment can be found in [13]. It may suffice to remark here that fixing a statically determinate substructure – by removing geometrical constraints at the perimeter and/or by cutting the enclosing frame – and defining the redundant forces are analogous to the treatment of framed structures by the Force Method.

For walls with openings which represent multiply-connected regions, the basic plate equation and the given external forces along the edges are not sufficient for the complete mathematical definition of the problem. For the wall shown in Fig. 3 the boundary conditions along the external contour are

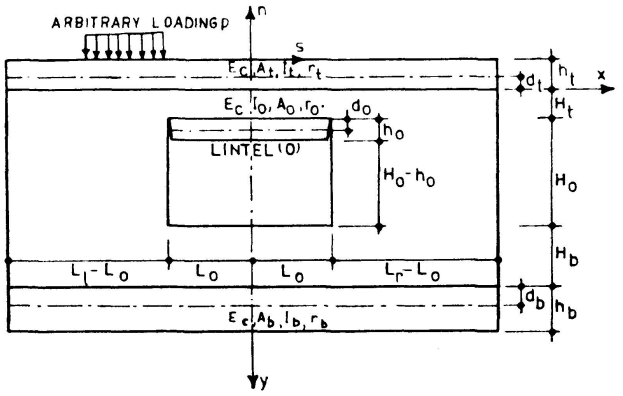

Fig. 3. Wall with single window opening.

the same as for the solid walls. Along the internal contour, in the absence of loads there, one has:

— for the two vertical and the lower horizontal edges:

$$\sigma_n = \tau = 0,$$

which by integration yield (Fig. 4);

$$\frac{\partial \Phi}{\partial y} = A_2, \qquad \frac{\partial \Phi}{\partial x} = A_3, \qquad \Phi = A_1 + A_2 (y - H_t) + A_3 x \tag{12}$$

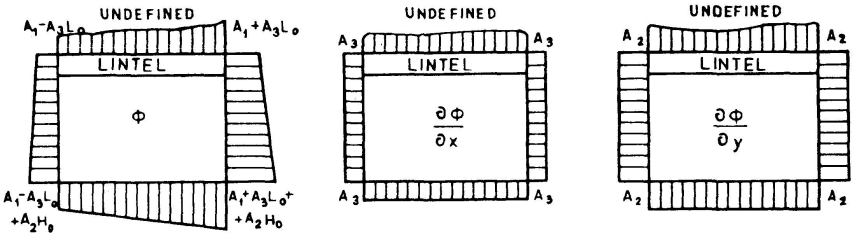

Fig. 4. Φ, $\frac{\partial \Phi}{\partial x}$ and $\frac{\partial \Phi}{\partial y}$ along inner perimeter.

— for the stiffened upper edge, the boundary conditions are anlogous to (6) and (7) in which:

$$\begin{aligned} N_e &= t\left(\frac{\partial \Phi}{\partial y}\right)_{L_0, H_t} = t A_2, \\ M_e &= t\left[d_0 \left(\frac{\partial \Phi}{\partial y}\right)_{L_0} + \Phi_{L_0, H_t} - (L - x)\left(\frac{\partial \Phi}{\partial x}\right)_{L_0, H_t}\right] = t\left[d_0 A_2 + A_1 + A_3 x\right]. \end{aligned} \tag{13}$$

Thus it can be seen that for the formulation of the boundary conditions the values of three generalized redundant forces $A_i (i = 1, 2, 3)$ are required.

If the wall is imagined to be cut through below the opening, the two cut edges undergo relative displacements as shown in Fig. 5. Castigliano's theorem yields the following relations between the strain energy U and the displacement components:

$$\frac{\partial U}{\partial A_1} = t\alpha_0, \qquad \frac{\partial U}{\partial A_2} = t(u_0 - \alpha_0 H_0), \qquad \frac{\partial U}{\partial A_3} = -t v_0, \tag{14}$$

which equalled to zero yield the redundants A_i.

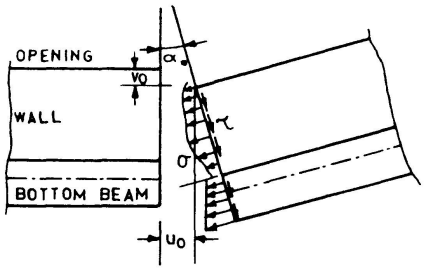

Fig. 5. Displacement components of edges.

In the analysis of statically indeterminate walls of any class one has to find a number of stress functions, namely for the external loading and for the unit values of the redundants, as indicated in the following table:

Symbol	*External load*	*Value of redundants*	*Stress function*
0	P (as given)	all zero	Φ_0
1	zero	$X_1 = 1;\ X_{i\neq 1} = 0$	Φ_1
2	zero	$X_2 = 1;\ X_{i\neq 2} = 0$	Φ_2
⋮	⋮	⋮	⋮
n	zero	$X_n = 1;\ X_{i\neq n} = 0$	Φ_n

The actual stress function is then $\Phi = \Phi_0 + \sum_{i=1}^{n} X_i \Phi_i$.

The equations for computing the redundants are:

$$\frac{\partial}{\partial X_j} U(P, X_1, X_2, \ldots, X_n) = 0, \qquad j = 1, 2, \ldots, n. \tag{14}$$

Without giving here the details of deduction, the integrals F_{ij} related to the unit values of the redundants and to the external loading are defined as follows:

$$F_{ij} = \frac{t}{E_w} \sum_{k=1}^{f} \int \left[\frac{\partial^2 \Phi_i}{\partial n^2} \frac{\partial \Phi_j}{\partial n} - \left(\frac{\partial^3 \Phi_i}{\partial n^3} + 2 \frac{\partial^3 \Phi_i}{\partial n \, \partial s} \right) \Phi_j \right] ds$$
$$+ \frac{1}{E_c} \left[\sum_{k=1}^{l} \frac{1}{I_k} \int (M_i M_{ej} + r_k^2 N_i N_{ej}) \, ds + \sum_{k=1}^{m} \frac{1}{A_k} \int N_i N_{ej} \, ds \right. \tag{15}$$

f, l, m denote the number of unstiffened edges, external and internal stiffeners, respectively.

For $j=0$, F_{i0} is the displacement vector $\{u\}$ due to external loads, and for $j \neq 0$ F_{ij} provides the flexibility matrix $[F]$ of the structure.

After calculating all values F_{ij} (taking advantage of the symmetry with respect to the matrix diagonal) the solution of the set of equations

$$\{u\}+[F]\{X\}=0 \tag{16}$$

yields the redundants X_j.

Numerical Solution and Computer Program

The numerical solution is based on the Finite Differences method. The different stages – transcription of the plate equation and of the boundary conditions into central finite differences for points of a grid, solution of the equations to obtain the stress function, determination of the stresses in the plate and of the internal forces in the stiffening elements by numerical differentiation of the stress function – do not contain any novel features and, therefore, are not detailed here. A computer program for one-storey walls with and without openings, with stiffening element in any position, and for any type of loading was written in Algol for an Elliott 503 computer [13].

A few representative examples of solution obtained are shown in Figs. 6–8.

Approximate Analysis

In the following the influence of certain parameters are discussed, and consequently, with the aid of the results obtained by numerical analysis, some formulae for approximate analysis are suggested. The proposed approximations regard mainly the most heavily stressed regions of solid walls in the vicinity of concentrated loads, including support reactions. The parameters discussed are: rigidity of the components (plate and stiffeners), wall height, continuity over intermediate supports, openings.

Rigidity of the components. The numerical solutions bring into relief the following findings (which could largely have been anticipated):

Stiffening post (external or internal) causes a drastic reduction of compression (σ_y) in the plate and of the bending moment in the bottom beam, because an essential part of the load is transferred directly by the post.

Between post and plate arise shear stresses which reduce the axial force in the post gradually from bottom to top.

Three different cases regarding the location of the external loads with respect to the stiffening elements shall be distinguished:

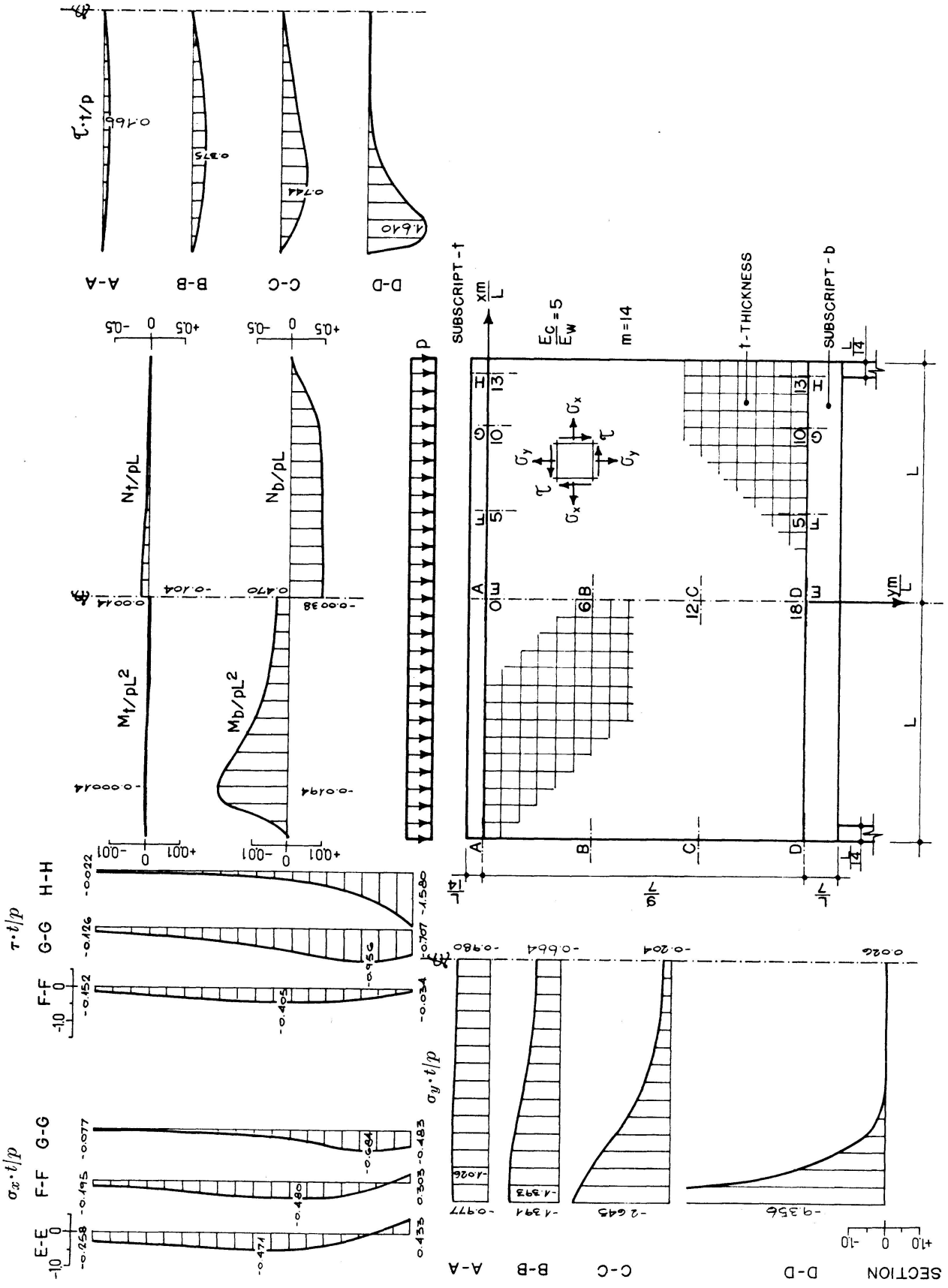

Fig. 6. Wall bordered by horizontal beams.

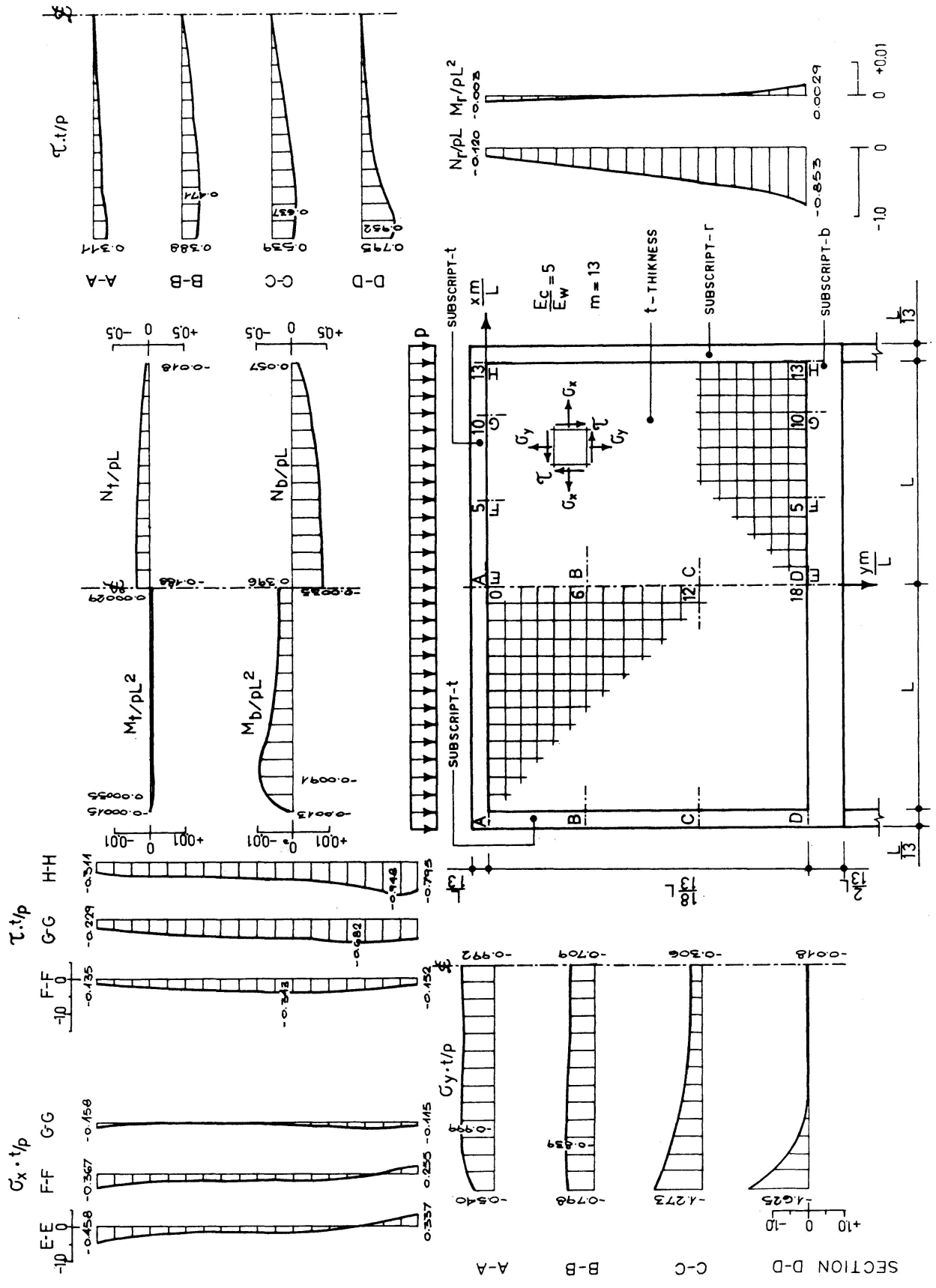

Fig. 7. Infilled frame.

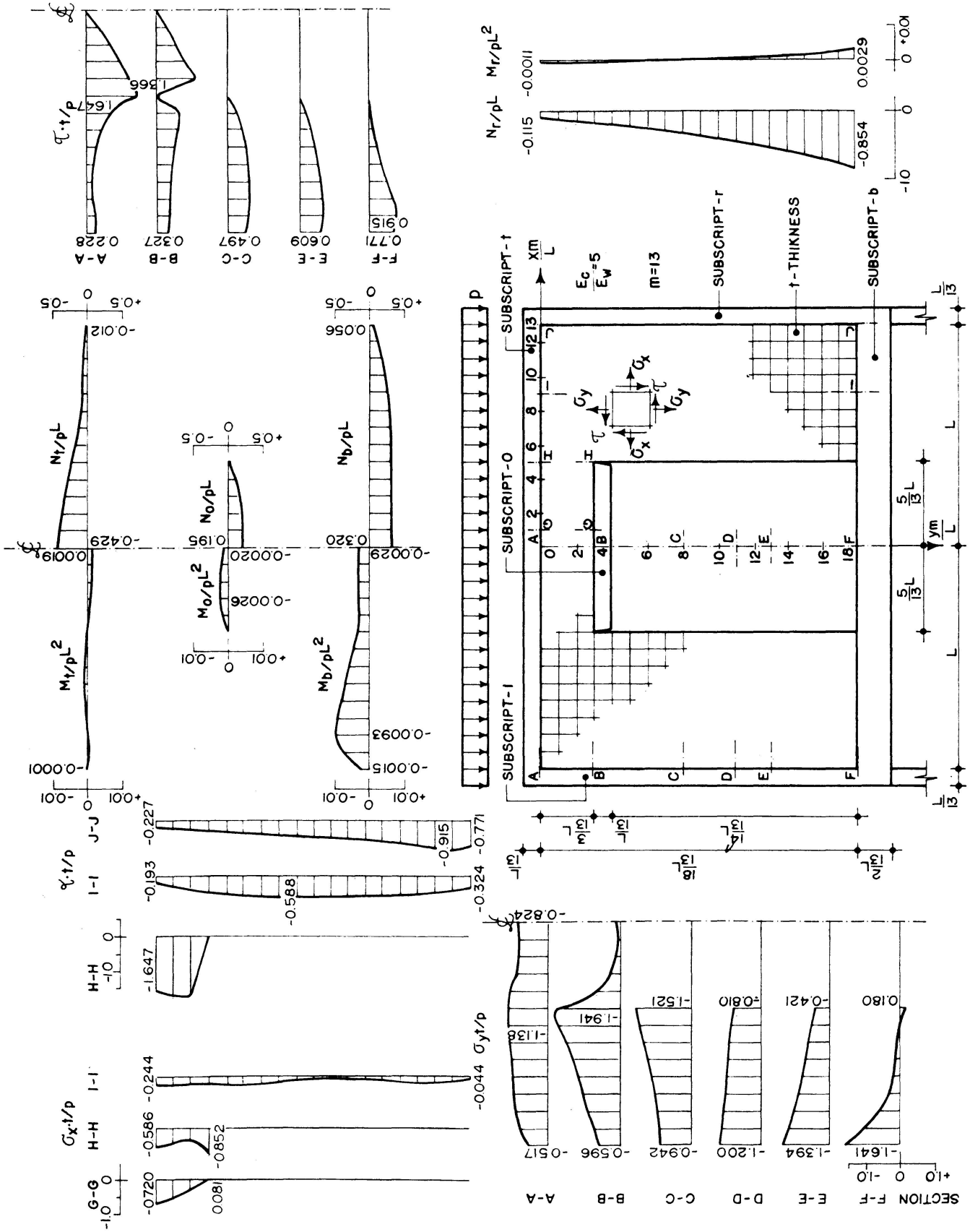

Fig. 8. Infilled frame with door opening.

a) *Load Acting Perpendicularly to the Stiffener*

A parameter K_1 can be identified, which has preponderant influence on the contact stresses, and shall be defined as such depth of plate which replacing the edge beam will leave the contact stresses σ_y unaltered (Fig. 9).

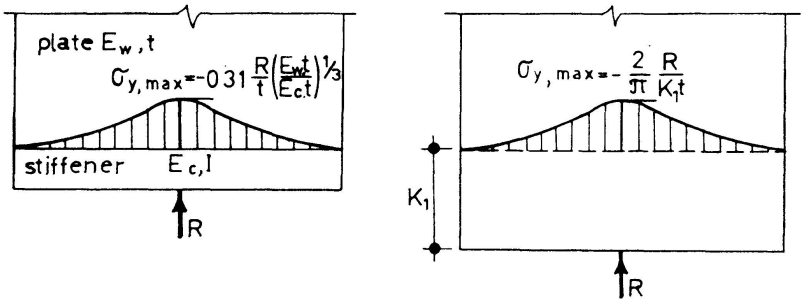

Fig. 9. Equivalent depth K_1.

K_1 is obtained by equating the maximal pressure exerted by a force R on the half-plane through a beam [3].

$$\sigma_{y,max} = -0.31\frac{R}{t}\left(\frac{E_w t}{E_c I}\right)^{1/3}$$

with that of a homogeneous half-plane at a depth K_1

$$\sigma_{y,max} = -\frac{2}{\pi}\frac{R}{t K_1},$$

so that

$$K_1 = 2\left(\frac{E_c I}{E_w t}\right)^{1/3}. \tag{17}$$

On the basis of the numerical results obtained for walls with bottom beams typical graphs were constructed for the non-dimensional statical values:

$$\bar{\sigma} = \sigma\frac{K_1 t}{R}, \qquad \bar{N} = \frac{N}{R}, \qquad \bar{M} = \frac{M}{R K_1}. \tag{18}$$

Such graphs, which are valid for reasonably long edges ($2L \geqq 8K_1$) are shown in Fig. 11 for loads acting near the corners and in Fig. 12 loads removed from the corners.

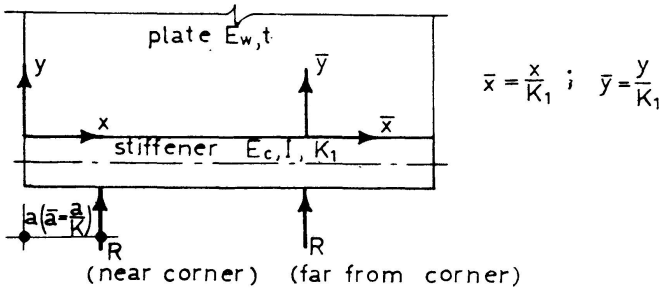

Fig. 10. Load perpendicular to edge beam.

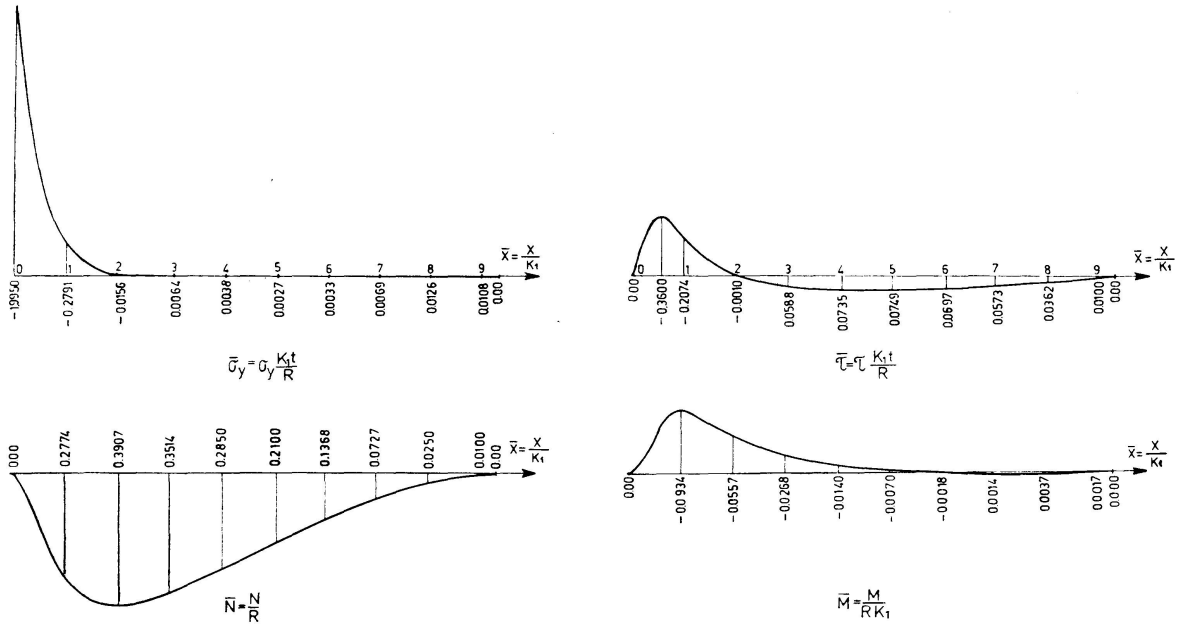

Fig. 11. Contact stresses and internal forces of beam due to load near corner $\left(\frac{a}{K_1} \approx 0.17\right)$.

Closed expressions approximating the above graphs were derived from the known stress formulae for the quarter-plane and the half-plane at a depth K_1 (Fig. 10):

for $0 \leqq \frac{a}{K_1} \leqq 1$

$$\begin{aligned} \bar{\sigma}_y &= \sigma_y \frac{K_1 t}{R} = \frac{4}{\pi^2 - 4} \frac{2\bar{x} - \pi}{(\bar{x}^2+1)^2} + \frac{2\bar{a}(1-3\bar{x}^2)}{(\bar{x}^2+1)^3}, \\ \bar{\tau} &= \tau \frac{K_1 t}{R} = \frac{4}{\pi^2 - 4} \frac{2\bar{x}^2 - \pi\bar{x}}{(\bar{x}^2+1)^2} + \frac{4\bar{a}\bar{x}(1-\bar{x}^2)}{(\bar{x}^2+1)^3}, \end{aligned} \tag{19}$$

for $4 \leqq \frac{a}{K_1} < \infty$

$$\bar{\sigma}_y = -\frac{2}{\pi} \frac{1}{(\bar{x}^2+1)^2}, \qquad \bar{\tau} = -\frac{2}{\pi} \frac{\bar{x}}{(\bar{x}^2+1)^2}. \tag{20}$$

By integration of the stresses, given by the above formulae, the internal forces of the edge beam are obtained:

for $0 \leqq \frac{a}{K_1} \leqq 1$

$$\begin{aligned} \bar{N} &= \frac{N}{R} = \frac{4}{\pi^2 - 4}\left(\frac{\pi}{2} + \frac{2\bar{x} - \pi}{2(\bar{x}^2+1)} - \arctan\bar{x}\right) - \frac{2\bar{a}\bar{x}^2}{(\bar{x}^2+1)^2}, \\ \bar{M} &= \frac{M}{RK_1} = -\bar{x} + \frac{4}{\pi^2 - 4}\left[\left(1 + \frac{\pi}{2}\bar{x}\right)\arctan\bar{x} - \bar{x}\right] + \frac{\bar{a}}{\bar{x}^2+1} + \bar{N}\frac{d}{K_1}, \end{aligned} \tag{21}$$

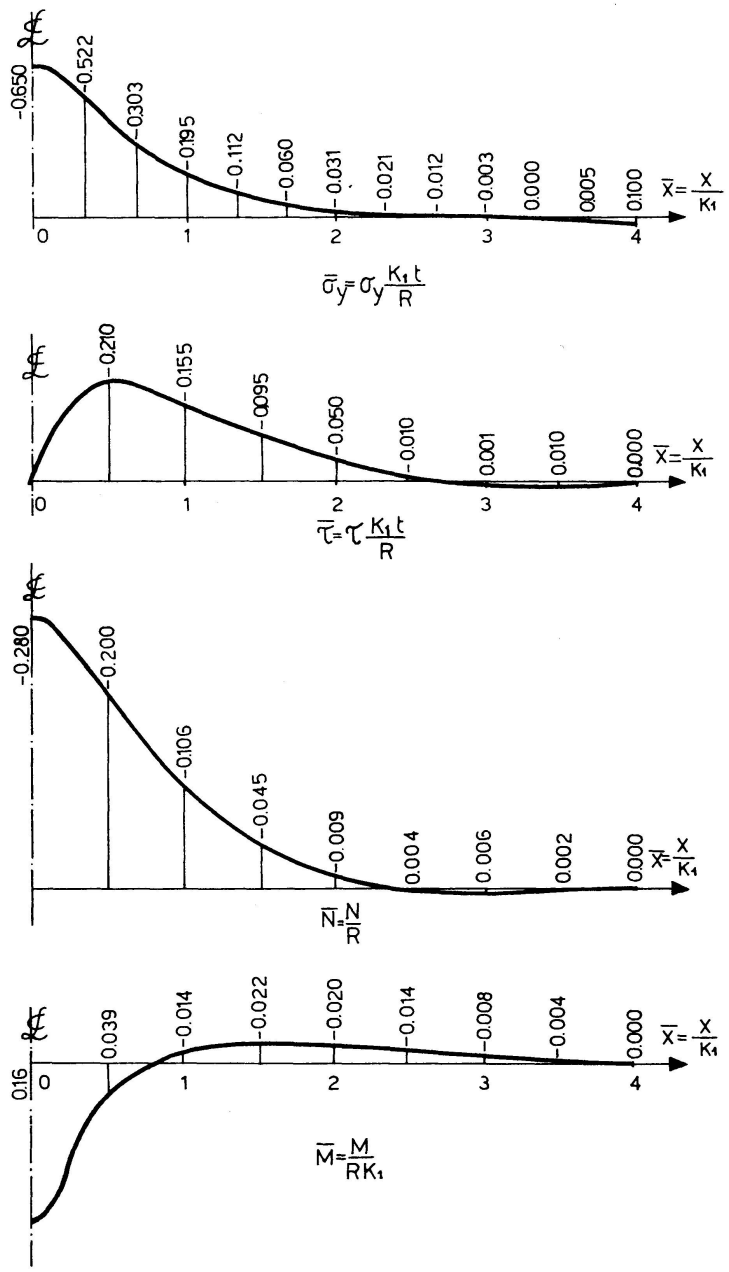

Fig. 12. Contact stresses and internal forces of beam due to load removed from corner $\left(\frac{a}{K_1}\approx 4\right)$.

for $4 \leqq \frac{a}{K_1} < \infty$

$$\bar{N} = -\frac{1}{\pi}\frac{1}{\bar{x}^2+1}, \qquad \bar{M} = \frac{1}{\pi}\left[1+\bar{x}\left(\arctan\bar{x}-\frac{\pi}{2}\right)\right]+\bar{N}\frac{d}{K_1}. \tag{22}$$

The agreement between the exactly calculated graphs and the approximating expressions is reasonably good, the maximal values differing within the limits of between 8 and 20 percent. The extremal values of the contact stresses and beam forces are summarized in Table 1.

Table 1. Extremal Values of Contact Stresses and Internal Forces of Beam for Perpendicular Load

	a=o		a ≥ 4K₁	
	Extremal Value	Its Location $\bar{x}$	Extremal Value	Its Location $\bar{x}$
$\sigma_y \frac{K_1 t}{R}$	-2.1	0	-0.65	0
$\tau \frac{K_1 t}{R}$	0.38	0.5	0.21	0.5
$\frac{N}{R}$	0.40	2	-0.28	0
$\frac{M}{RK_1}$	-0.10	1.0	0.16	0

b) *Load Acting in Line with the Axis of the Stiffening Element (Fig. 13)*

The numerical solutions show bending moments of the stiffening element in such cases to be negligible, which implies also the neglect of the perpendicular contact stresses. So the problem is reduced to that of finding the shear stress along the contact face and the axial force N in the stiffening element.

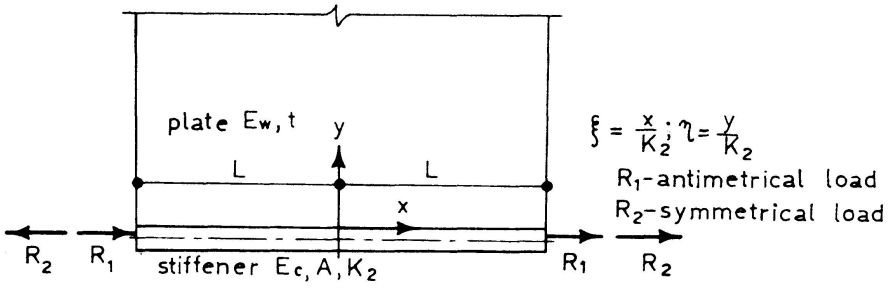

Fig. 13. Load acting in line with stiffener axis.

It may be assumed that these depend mainly on a parameter K_2, which expresses the relative axial rigidity.

$$K_2 = \frac{E_c A_c}{E_w t}. \tag{23}$$

For the derivation of approximate expressions for τ and N a wall of infinite height is considered which is bordered by a horizontal edge element with an axial load R. The following derivation makes use of the variational method of L. V. KANTOROVICH [5]. It will be performed separately for an antimetric and a symmetric load case.

Antimetry. The axial force in the edge element is:

$$N = t\left(\frac{\partial \Phi}{\partial y}\right)_{x,0}. \tag{24'}$$

The boundary conditions along the vertical (unstiffened) edges are

$$\left(\frac{\partial \Phi}{\partial x}\right)_{\pm L,y} = 0, \qquad \left(\frac{\partial \Phi}{\partial y}\right)_{\pm L,y} = \pm\frac{R}{t}, \qquad (\Phi)_{\pm L,y} = \pm\frac{R}{t}y. \tag{25'}$$

The compatibility conditions along the contact face (in the absence of perpendicular external loads) yield

$$\left(\frac{\partial \Phi}{\partial y} - K_2 \frac{\partial^2 \Phi}{\partial y^2}\right)_{x,0} = 0, \qquad (\Phi)_{x,0} = 0. \tag{26'}$$

Using the non-dimensional variables

$$\begin{aligned} \xi &= \frac{x}{K_2}, & \eta &= \frac{y}{K_2}, & n &= \frac{L}{K_2}, \\ \bar{\Phi} &= \Phi \frac{t}{R K_2}, & \bar{\sigma} &= \sigma \frac{K_2 t}{R}, & \bar{N} &= \frac{N}{R}, \end{aligned} \tag{27'}$$

the expressions (24), (25) and (26) read

$$\bar{N} = \left(\frac{\partial \bar{\Phi}}{\partial \eta}\right)_{\xi,0}, \tag{24}$$

$$\left(\frac{\partial \bar{\Phi}}{\partial \xi}\right)_{\pm n,\eta} = 0, \qquad \left(\frac{\partial \bar{\Phi}}{\partial \eta}\right)_{\pm n,\eta} = \pm 1, \qquad (\bar{\Phi})_{\pm n,\eta} = \eta, \tag{25}$$

$$\left(\frac{\partial \bar{\Phi}}{\partial \eta} - \frac{\partial^2 \bar{\Phi}}{\partial \eta^2}\right)_{\xi,0} = 0, \qquad (\bar{\Phi})_{\xi,0} = 0. \tag{26}$$

The following expressions are obtained (their derivations are given in [13]).

$$\begin{aligned} \bar{\tau} &= \tau \frac{K_2 t}{R} = \frac{3}{2n}\left(\frac{\xi^2}{n^2} - 1\right) + \frac{n}{n+\pi}\left(\frac{\pi}{2n}\cos\frac{\pi\xi}{2n} + \frac{da}{d\xi}\right), \\ \bar{N} &= \frac{N}{R} = \frac{1}{2}\left(3\frac{\xi}{n} - \frac{\xi^3}{n^3}\right) - \frac{n}{n+\pi}\left(\sin\frac{\pi\xi}{2n} + a(\xi)\right), \end{aligned} \tag{27}$$

in which

$$\begin{aligned} a(\xi) &= C_1 \phi_1(\xi) + C_2 \phi_2(\xi), \\ \frac{da}{d\xi} &= (C_2\lambda_1 - C_1\lambda_2)\phi_3(\xi) + (C_1\lambda_1 + C_1\lambda_2)\phi_4(\xi). \end{aligned} \tag{28}$$

the functions $\phi_1 \div \phi_4$ are defined as follows

$$\begin{aligned} \phi_1(\xi) &= \operatorname{sh}\lambda_1\xi\cos\lambda_2\xi, & \phi_2(\xi) &= \operatorname{ch}\lambda_1\xi\sin\lambda_2\xi, \\ \phi_3(\xi) &= \operatorname{sh}\lambda_1\xi\sin\lambda_2\xi, & \phi_4(\xi) &= \operatorname{ch}\lambda_1\xi\cos\lambda_2\xi, \\ \lambda_1 &= \frac{1}{2}\frac{\pi}{n}\left(\frac{\gamma+1}{2}\right)^{1/2}, & \lambda_2 &= \frac{1}{2}\frac{\pi}{n}\left(\frac{\gamma-1}{2}\right)^{1/2}, & \gamma &= \left(\frac{8n}{\pi}+5\right)^{1/2}. \end{aligned} \tag{29}$$

The values of C_i in (28) are determined from the boundary conditions

$$a(n) = -1, \qquad \left(\frac{da}{d\xi}\right)_{\xi=n} = 0,$$

which lead to the following pair of equations.

$$\begin{aligned} C_1\Phi_1(n) + C_2\Phi_2(n) &= -1, \\ C_1[\lambda_1\Phi_4(n) - \lambda_2\Phi_3(n)] + C_2[\lambda_1\Phi_3(n) + \lambda_2\Phi_4(n)] &= 0. \end{aligned} \tag{30}$$

Symmetry. The boundary conditions (in non-dimensional formulation) are:

$$\left(\frac{\partial\bar{\Phi}}{\partial\xi}\right)_{\pm n,\eta} = \left(\frac{\partial\bar{\Phi}}{\partial\eta}\right)_{\pm n,\eta} = (\bar{\Phi})_{\pm n,\eta} = 0,$$
$$\left(\frac{\partial\bar{\Phi}}{\partial\eta} - \frac{\partial^2\bar{\Phi}}{\partial\eta^2}\right) = -1, \qquad (\bar{\Phi})_{\xi,0} = 0. \tag{31}$$

The following approximate formulae can be written for the symmetrical case

$$\bar{\tau} = \tau\frac{K_2 t}{R} = -\frac{0.6504\,\pi^2}{(n+2\pi)(n+1.3496\,\pi)}\sin\frac{\pi\xi}{n} - \frac{n}{n+2\pi}\frac{da}{d\xi},$$
$$\bar{N} = \frac{N}{R} = \frac{1.3496\,\pi}{n+1.3496\,\pi} - \frac{0.6504\,\pi n}{(n+2\pi)(n+1.3496\,\pi)}\cos\frac{\pi\xi}{n} + \frac{n}{n+2\pi}a(\xi), \tag{32}$$

in which

$$a(\xi) = C_1\phi_1(\xi) + C_2\phi_2(\xi),$$
$$\frac{da}{d\xi} = (C_1\lambda_2 + C_2\lambda_1)\phi_3(\xi) + (C_1\lambda_1 - C_2\lambda_2)\phi_4(\xi). \tag{33}$$

The functions $\phi_1 \div \phi_4$ are defined as follows:

$$\phi_1(\xi) = \operatorname{sh}\lambda_1\xi\sin\lambda_2\xi, \qquad \phi_2 = \operatorname{ch}\lambda_1\xi\cos\lambda_2\xi,$$
$$\phi_3(\xi) = \operatorname{sh}\lambda_1\xi\cos\lambda_2\xi, \qquad \phi_4 = \operatorname{ch}\lambda_1\xi\sin\lambda_2\xi,$$
$$\lambda_1 = \frac{\pi}{n}\left(\frac{\gamma+1}{2}\right)^{1/2}, \qquad \lambda_2 = \frac{\pi}{n}\left(\frac{\gamma-1}{2}\right)^{1/2}, \qquad \gamma = \left(\frac{4n}{\pi}+5\right)^{1/2}. \tag{34}$$

The values of C_i in (33) are determined from the boundary conditions

$$a(n) = 1, \qquad \left(\frac{da}{d\xi}\right)_{\xi=n} = 0,$$

which lead to the following pair of equations

$$C_1\phi_1(n) + C_2\phi_2(n) = 1,$$
$$C_1[\lambda_1\phi_4(n) + \lambda_2\phi_3(n) + C_2(\lambda_1\phi_3(n) - \lambda_2\phi_4(n)] = 0. \tag{35}$$

The graphs in Fig. 14a show the contact shear stresses and the axial force due to an antimetric force for $n = 1.4$.

In the case of eccentricity of line of action the solution can be obtained by the superposition of the results for axial action and for the eccentricity moment – Re – whose effect can approximately be expressed by the terms containing (a) in formulae (19), (21).

Fig. 14b shows the contact shear and the axial force for the case of the external force acting at the level of the free edge of the stiffener $e/K_2 = 0.10$; full lines show the approximations, dotted lines those obtained by full numerical analysis. Except for some discrepancy in the vicinity of the point of application of the external force, which seems to be mainly due to the above

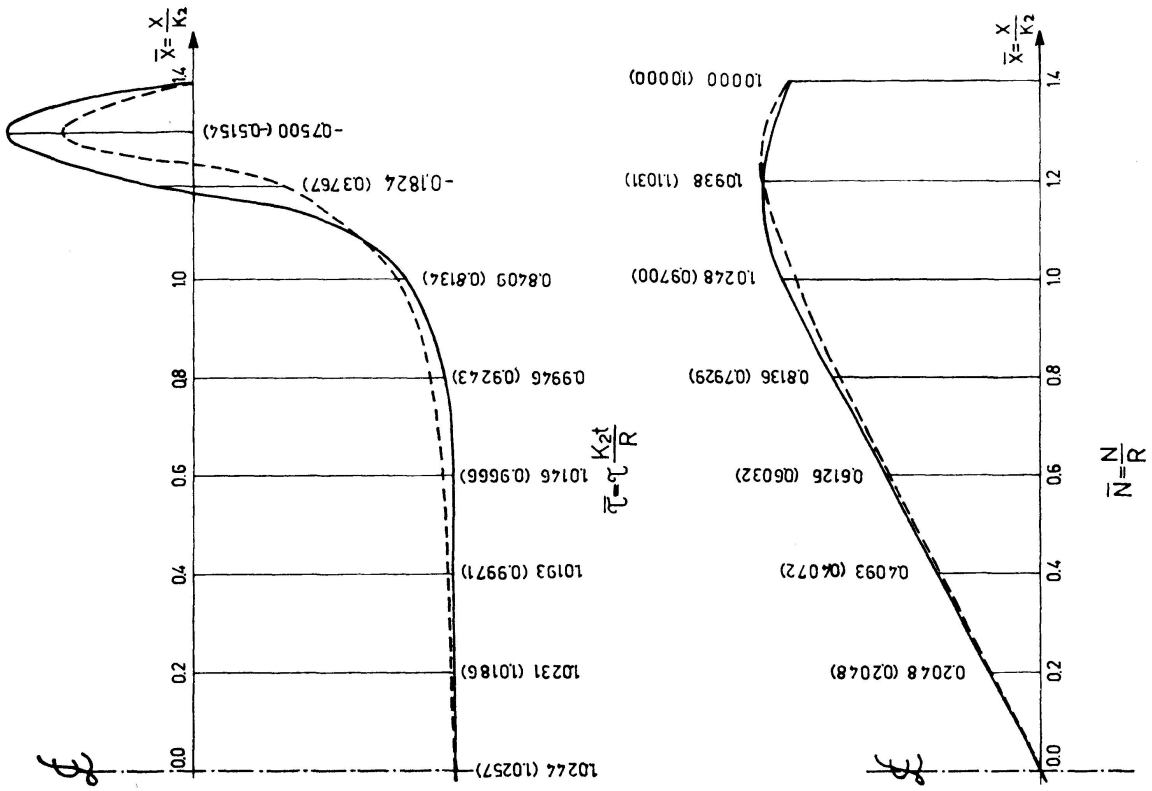

(b) Load acting with eccentricity $\frac{e}{K_2} = 0.10$.

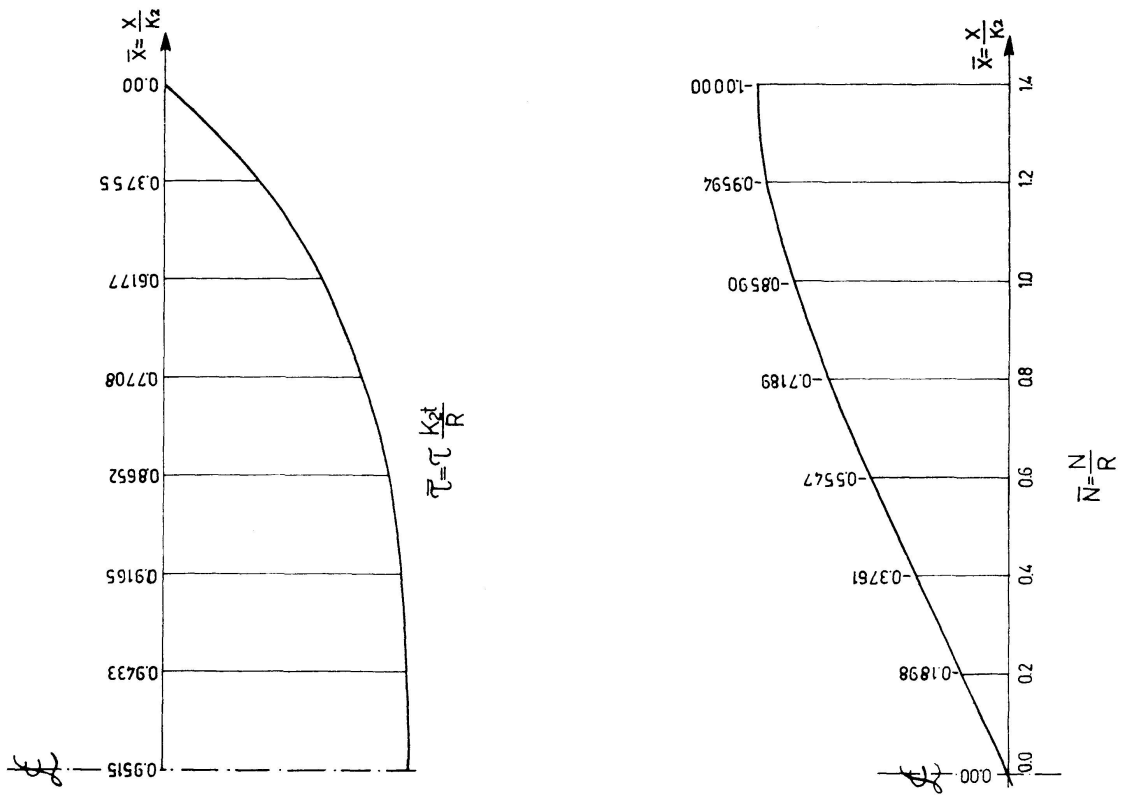

(a) Load acting in line with stiffener.

Fig. 14. Contact shear stresses and axial force for $n = \frac{L}{K_2} = 1.4$.

indicated treatment of the eccentricity, the agreement appears to be satisfactory.

It should be noted that with increasing K_2 and decreasing n, i.e. for increasing axial rigidity of the stiffening element, the graph of the contact shear stress becomes parabolic similar to the shear stress in ordinary slender beams, whereas with decreasing rigidity it flattens out.

c) *Loads Acting at Frame Corners*

The main problem here is to determine that part of the concentrated load which is transferred into the column (N_{col}). The column shall be assumed to receive axial loads only. N_{col} is applied at the faces of an imaginary cut (see Fig. 15), and its value will be obtained from the equation of vertical strains of wall ϵ_w and column ϵ_{col}.

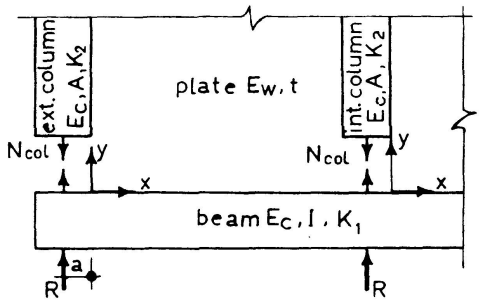

Fig. 15. Load acting at frame joint.

According to (19) and (20):

$$\epsilon_w = C\frac{R+N_{col}}{K_1 t E_w}, \quad \text{in which } C = -\frac{4\pi}{\pi^2-4} - \frac{2a}{K_1} = -2.14 - \frac{2a}{K_1},$$

if the load is close to the corner; but $C = -\frac{2}{\pi} = -0.64$ if it is far from the corner.

The strain in the column is $\frac{N_{col}}{E_c A_c}$.

Now, the condition $\epsilon_{col} = \epsilon_w$ yields:

$$\frac{N_{col}}{R} = \frac{CK_2}{K_1 - CK_2}. \tag{36}$$

According to the derivation, the approximate maximal value of the contact stress σ_y appears to be:

$$\sigma_{y,max} = C\left(1+\frac{N_{col}}{R}\right)\frac{R}{K_1 t}. \tag{37}$$

The authors have not been able to propose a reliable formula for the internal forces of the stiffening beams. But with some reservation it may be suggested that with frame columns present N in the bottom beam is by 20% and M by 40–60% smaller than those without columns.

In conclusion of this paragraph the following should be noted:

— The approximation formulae stated may generally suffice for the design of load bearing walls without opening, i.e. for designing the section of the bottom beam and checking the maximal plate stresses.
— The above formulae were, for the most part, derived from the half-plane and quarter-plane. Their usefulness is, therefore, limited to "tall" walls.
— For the use of the above formulae the knowledge of the external forces along the perimeter, including redundant support reactions, is required. The following two paragraphs deal with these questions.

The effect of height. A load-bearing wall with a bottom beam shall be defined as "tall" if any increase in plate height – H – does not appreciably change the contact stresses and the internal forces of the beam. Let H_t denote the limit value of "tall" wall.

In order to arrive at a numerical value for H_t the maximal contact stresses obtained from numerical analysis were compared with correspondent values given in table 1.

For walls with $4.5 \leqq \frac{H}{K_1} \leqq 6.5$ deviations were less than 5%; for $\frac{H}{K_1} \approx 3.3$ the deviations were 5%–8%, and in the range $1.8 \leqq \frac{H}{K_1} \leqq 2.5$ the deviations exceeded 20%.

Thus it may be concluded that $H_t = 4\,K_1$ and for walls with $\frac{H}{K_1} \geqq 4$ approximating formulae of the preceding paragraph are applicable. It may be noted that many of the common structures belong to this category.

Continuity over internal supports. Some examples of continuous walls, which were numerically analyzed, are shown in Fig. 16 and the internal support reactions indicated. In these examples, with $\frac{H}{K_1} > 4$ and $\frac{H}{L} > 0.65$, the distribution of the reactions is similar to that of beams with hinges over the supports, i.e. there is *no appreciable increase of the internal reactions* on account of continuity. This, in fact, applies, to a certain measure, also to homogeneous deep beams and is due to the strain effect of the σ_y and τ stresses (negligible in slender beams). The cumulative compression in the vicinity of the supports due to σ_y appears to be particularly pronounced in composite walls.

On the strength of this, the indeterminacy problem of continuous walls may often be bypassed by directly estimating the reaction forces, and an approximate analysis may be initiated from there.

The effect of wall openings. The numerical solution obtained tends to indicate that the stress distribution in the support areas is not appreciably different for walls with openings compared with that of solid walls. It is, however, substantially different at some distance from the supports.

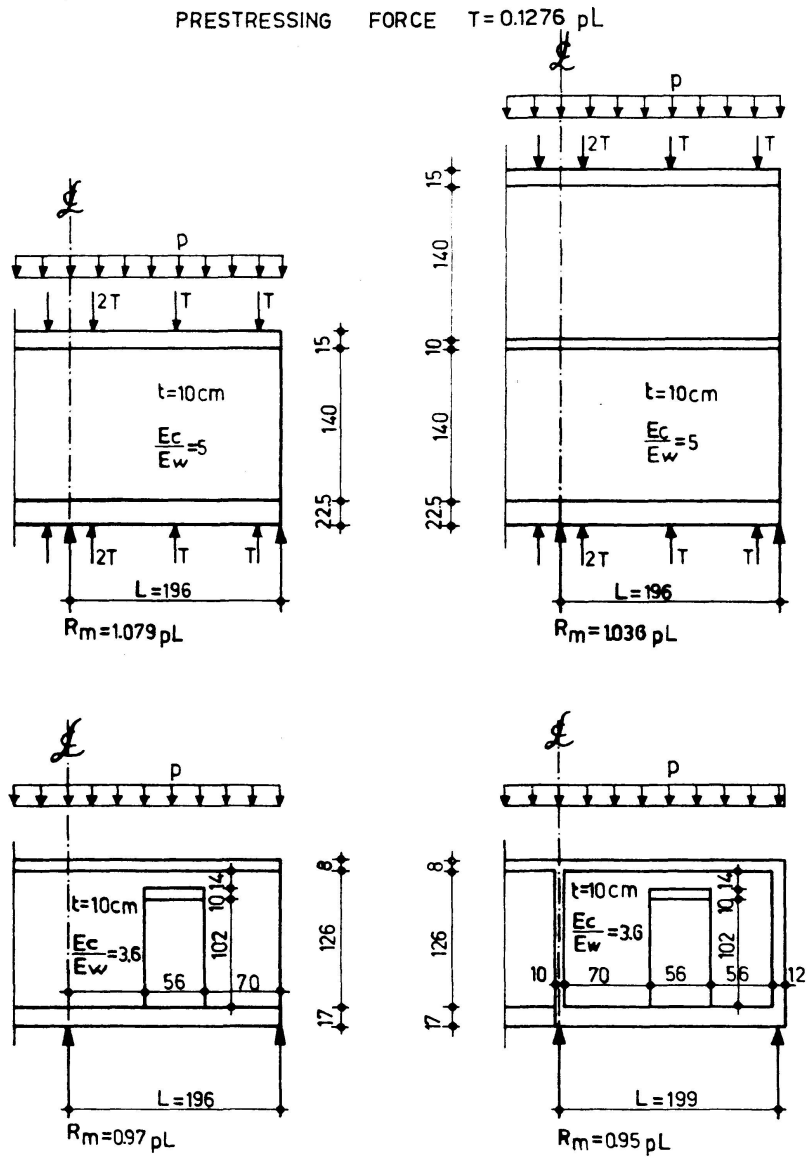

Fig. 16. Redundant reactions of continuous composite walls.

Qualitatively the following may be stated as regards the effect of a wall opening:

a) In a symmetrical case (regarding loading and position of openings) the integral shear is carried mainly by that part of the walls (above or below the openings) which is nearer to the load. If the non-loaded part is the beam only, then the shear force in it is zero.

Obviously, the wall part loaded by greater shear carried also the larger part of bending moment and the horizontal stresses reach high values.

In the less loaded wall parts, the stresses remained even below those of solid walls.

b) In antimetrical loadings the integral shear splits, proportionally to the stiffness of the wall parts above and below the opening.

The design requires checking of stresses in the lintel and the plate in the vicinity of the opening. No ready-to-use formulae could be developed for this purpose.

It might, in principle, be possible after splitting (analogously to frame analysis) the integral forces into parts related to wall parts above and below the opening, to deal with those parts as with ordinary or deep beams, depending on their slenderness.

Conclusions

In the analysis of composite walls described in this paper, the contact problem and the plate stresses could be solved by a continuous procedure in consequence of an appropriate formulation of the boundary conditions.

The method is based on the determination of stress function values by the finite differences method and it is, therefore, specially suitable for composite walls having a low degree of statical indeterminacy.

In the present article only isotopic plates were treated, but the method can readily be extended to orthotopic plates bordered by stiffening elements.

On the basis of the numerical analysis of a considerable number of cases, the influence of some important parameters was investigated with the aim of formulating simple design procedures.

Notation

A cross sectional area of stiffener

a distance of concentrated load from wall corner

$a(\xi)$ function of ξ – Eq. (28), (33)

$A_1 \div A_3$ generalized redundant forces in walls with openings, Eq. (12), (13)

C_1, C_2 integration constants, Eq. (30), (35)

d distance of stiffener axis from wall edge

E_c, E_w modulus of elasticity of stiffener and wall, respectively

$[F]$ flexibility matrix, Eq. (16)

I moment of inertia of stiffener

H height of wall

h depth of stiffener

K_1, K_2 relative bending and axial rigidity of stiffener, Eq. (17), (23)

L half length of wall

$M, \overline{M}$ bending moment in stiffener (tension at inside fibres-positive) and non-dimensional notation, $\overline{M} = \frac{M}{RK_1}$

M_e bending moment in stiffener due to external load

m_e external distributed moment

$N, \bar{N}$ axial force in stiffener (tension-positive), and non-dimensional notation, $\bar{N} = \frac{N}{R}$

N_e axial force in stiffener due to external load

n normal coordinate (positive outwards) or constant $n = \frac{L}{K_2}$

R concentrated load

r radius of gyration

s circumferential coordinate (positive clockwise)

t wall thickness

U strain energy

u, v longitudinal and transverse displacement along stiffened wall edges, respectively, or horizontal and vertical relative displacement between cut edges

$\{u\}$ displacement vector

$\{X\}$ redundant – force vector

$X, \tilde{X}$ horizontal distributed external and contact forces

$Y, \tilde{Y}$ vertical distributed external and contact forces

x, y Cartesian coordinates; non-dimensional notation – $\bar{x} = \frac{x}{K_1}, \bar{y} = \frac{y}{K_1}$

α angle between cut edges

ξ, η nondimensional coordinates – $\xi = \frac{x}{K_2}$, $\eta = \frac{y}{K_2}$

λ_1, λ_2 constants – Eq. (29), (34)

$\sigma, \bar{\sigma}$ normal stress, and nondimensional notation – $\bar{\sigma} = \sigma \frac{K_1 t}{R}$ or $\bar{\sigma} = \sigma \frac{K_2 t}{R}$

$\tau, \bar{\tau}$ shear stress, and nondimensional notation – $\bar{\tau} = \tau \frac{K_1 t}{R}$ or $\bar{\tau} = \tau \frac{K_2 t}{R}$

$\Phi, \bar{\Phi}$ Airy stress function, and nondimensional notation, $\bar{\Phi} = \Phi \frac{t}{R K_2}$

$\phi_1 - \phi_4$ functions of ξ – Eq. (29), (34)

Subscripts

c of stiffener

l, r of left-hand and right-hand sides of internal stiffener

o of opening

w of wall

Acknowledgements

A considerable part of the proposed method was worked out in the thesis presented by M. Levy to the Senate of the Technion-Israel Institute of Technology, in February 1967, in partial fulfilment of the requierments for the degree of Doctor of Science in Technology.

This method was further extended and applied to the numerical solution of various practical problems in a theoretical and experimental research dealing with masonry walls bordered by reinforced concrete stiffeners.

The authors wish to express their gratitude to the U.S. National Bureau of Standards, who sponsored the above-mentioned project.

Thanks are also due to the Israel Ministry of Housing, who supported a number of projects in connection with the thesis work.

Keywords

Wall, stiffener; stress function; boundary conditions; composite construction; finite differences; computer; approximate analysis.

References

[1] Boardman, V. R.: Reinforcement of Brick Walls to Reduce Cracking on Heaving Foundations. C.S.I.R. – National Building Research Institute (Pretoria), Bulletin No. 14, 1956, March.

[2] Ghali, A. and Bathe, K. J.: Analysis of Plates Subjected to In-Plane Forces Using Large Finite Elements. Publications, I.A.B.S.E., Zurich, Vol. 30 (1970) I, p. 61–72.

[3] Girkmann, K.: Flächentragwerke. 4. Auflage, Springer, Vienna, 1956.

[4] Gruning, G.: Beitrag zum Spannungsbild des wandartigen Trägers. Bauplanung – Bautechnik, 10. Jg., Heft 8, August 1956, VEB Verlag Technik, Berlin.

[5] Kantorovich, L. V. and Krylov, V. I.: Approximate Methods of Higher Analysis. Nordhoff, Groningen, 1959.

[6] Levy, M.: Analysis of Wall Panels Bordered by Stiffening Elements. D. Sc. Thesis, Technion, Haifa, February 1967 (in Hebrew).

[7] Mallick, D. V. and Garg, R. P.: Effects of Openings on the Lateral Stiffness of Infilled Frames. Inst. Civ. Engrs. Proc. 49, June 1971, p. 193–209.

[8] Pian, T. H. H. and Tong, P.: Basis of Finite Elements Methods for Solid Continua. International Journal for Numerical Methods in Engineering, 1969, p. 3–28.

[9] Pollner, E.: Analysis of Composite Orthotropic Shear Walls. D. Sc. Thesis, Technion, Haifa, January 1970 (in Hebrew).

[10] Popova, T. A.: Some Problems on Behaviour of Plates with Rectangular Openings – Research on Strength, Stiffness and Stability of Large Panel Construction. Stroizdat 1964 (in Russian).

[11] Rosenhaupt, S.: Stresses in Point Supported Composite Walls. ACI Jour. 61, No. 7, 1964, p. 795–810.

[12] Rosenhaupt, S. and Mueller, G.: Opening in Masonry Walls on Settling Supports. Journal of the Structural Division, ASCE, Vol. 89, No. ST 3, June, 1963, p. 107–131.

[13] Spira, E. and Levy, M.: Stress Analysis of Composite Walls and Walls with Openings. Final report to U.S. National Bureau of Standards, Building Research Station, Technion, Haifa, November 1970.

[14] Stafford-Smith, B.: The Composite Behaviour of Infilled Frames. Proc. of Symposium on Tall Buildings, Southampton 1966, Pergamon (1967).

[15] Wood, R. H.: Studies in Composite Construction. Part 1. Nat. Building Study, Research Paper No. 13, London, H.M.S.O., 1952.

[16] Zhemochkin, V. N.: Analysis of Supporting Beams and Bearing Walls. Gosstroizdat, 1960 (in Russian).

Summary

A numerical method is presented for elastic analysis of load-bearing walls strengthened by stiffeners, based on determination of the Airy stress function by the finite-differences technique. Judicious formulation of the boundary conditions along the strengthened wall edges permitted the contact problem, and the in-plane stress distribution in the plate, to be solved by a continuous procedure.

The computer program yields the in-plane stress components in the plate and the internal forces along the stiffeners.

On the basis of the numerical analysis of a considerable number of particular cases, the influence of some important parameters was investigated with the aim of formulating simple design procedures.

Résumé

On présente une méthode numérique pour l'analyse élastique des parois renforcées par raidisseurs se basant sur la détermination de la fonction de contraintes Airy moyennant la technique des différences finies. Une formulation judicieuse des conditions-limites le long des bords sollicités des parois a permis de résoudre le problème de contact et la distribution de la sollicitation dans la paroi moyennant un procédé continu.

Le programme d'ordinateur donne les composantes dans le plan des parois et les forces internes le long des raidisseurs.

Sur la base d'une analyse numérique d'un grands nombre de cas particuliers l'influence de quelques paramètres importants fut examinée afin de formuler de simples procédés de projet.

Zusammenfassung

Es wird eine numerische Methode zur elastischen Analyse von tragenden, durch Versteifungen verstärkten Wänden vorgelegt, die auf der Bestimmung der Airy-Spannungfunktion mittels Differenzenrechnung basiert. Eine zweckentsprechende Formulierung der Grenzbedingungen längs der beanspruchten Wandkanten erlaubte das Kontaktproblem und die in der Wandebene liegende Verteilung der Beanspruchung mittels eines kontinuierlichen Verfahrens zu lösen.

Das Computerprogramm ergibt die in der Wandebene liegenden Komponenten und die inneren Kräfte längs der Versteifungen.

Auf Grund der numerischen Analyse einer erheblichen Anzahl besonderer Fälle wurde der Einfluss einiger wichtiger Parameter untersucht, um einfache Entwurfsverfahren zu formulieren.